J. Fluid Mech. (1984), *vol.* 140, *pp.* 45–61
Printed in Great Britain

A simple turbulence closure hypothesis for the triple-velocity correlation functions in homogeneous isotropic turbulence

By J. A. DOMARADZKI† AND G. L. MELLOR
Geophysical Fluid Dynamics Program, Princeton University, New Jersey 08540

(Received 7 February 1983 and in revised form 6 October 1983)

A simple two-point closure scheme for homogeneous axisymmetric turbulence is developed. For the isotropic case it is essentially an eddy-viscosity assumption in real space for the Kármán–Howarth equation. The eddy-viscosity function for large internal Reynolds numbers is derived from Kolmogoroff's 1941 theory. For moderate Reynold's numbers of order 10^2, approximately the same expression for the eddy-viscosity function is determined from experimental data. The resulting closed equation for the double-correlation function is solved numerically for both large and moderate Reynolds numbers, and the results are compared with experimental data. Self-similar solutions of the basic equation predict turbulent energy decay inversely proportional to time. It is shown that the departure from this 'initial-period decay law' observed in laboratory data is due to the behaviour of grid-produced correlation functions for large separation distances.

1. Introduction

The fundamental problem in the theory of turbulence is closure of equations describing the time evolution of different correlation functions of the turbulent field. A variety of closure schemes are described, for example, by Batchelor (1953), Hinze (1959), Monin & Yaglom (1971, 1975) and Rose & Sulem (1978). For isotropic turbulence, eddy-viscosity assumptions have been formulated in spectral space, and a survey of different possible assumptions may be found in Monin & Yaglom (1975). Much less attention has been directed to the formulation of eddy-viscosity concepts in real space coordinates. The paper by Hasselmann (1958) is, apparently, an exception. In the present paper we introduce a simple closure scheme for homogeneous axisymmetric turbulence which for the isotropic case is equivalent to an eddy-viscosity assumption in real space for the Kármán–Howarth equation. The exact form of the eddy-viscosity function is derived in §3 from Kolmogoroff's 1941 theory and from experimental data. The postulated closure relation between double- and triple-correlation functions seems to be much less dependent on Reynolds number than the correlation functions themselves. In §4 the theory is compared with experimental data for both high and moderate Reynolds numbers. Finally, in §5 the model is used to investigate the problem of the decay of turbulence, and we arrive at the conclusion that the energy decay rate is related to the behaviour of the correlation functions for large separation distances; specifically, an energy-decay rate inversely proportional to time, known as the initial-period decay law, requires that the initial double-correlation function behave as $1/r^2$ for large distances r. This result agrees with

† Permanent address: Institute of Geophysics, Warsaw University, Poland.

spectral results (Orszag 1977; Lesieur & Schertzer 1978)) which yield the initial-period decay law, assuming that the energy spectrum is linear in wavenumber k in the vicinity of $k = 0$. Laboratory data do not generally satisfy this condition and therefore depart from the initial-period decay law. Section 6 is devoted to the discussion of these results.

2. The closure assumption

Consider an incompressible fluid of constant density ρ. The velocity field $U_i(\boldsymbol{x}, t)$ satisfies the Navier–Stokes and continuity equations

$$\frac{\partial}{\partial t} U_i + U_\alpha \frac{\partial}{\partial x_\alpha} U_i = -\frac{1}{\rho}\frac{\partial}{\partial x_i} P + \nu \frac{\partial^2}{\partial x_\alpha \partial x_\alpha} U_i, \tag{1a}$$

$$\frac{\partial}{\partial x_\alpha} U_\alpha = 0. \tag{1b}$$

Here P and ν are the pressure and the kinematic viscosity respectively. Repeated lower indices imply summation. Velocity and pressure are decomposed into mean and turbulent parts

$$U_i(\boldsymbol{x}, t) = \overline{U}_i(\boldsymbol{x}, t) + u_i(\boldsymbol{x}, t), \tag{2a}$$

$$P(\boldsymbol{x}, t) = \overline{P}(\boldsymbol{x}, t) + p(\boldsymbol{x}, t), \tag{2b}$$

where the overbar denotes the average value. In what follows, we assume that the turbulent field is homogeneous and axisymmetric, i.e. two-point characteristics of turbulence depend only on a vector connecting these points and are invariant for rotations about preferred direction and for reflections in planes parallel and perpendicular to the axis of symmetry.

Equation (1) and the decomposition (2) in a homogeneous case leads to the following equations (Hinze 1959):

$$\partial_t \overline{U}_i + \overline{U}_\alpha \frac{\partial}{\partial x_\alpha} \overline{U}_i = -\frac{1}{\rho}\frac{\partial}{\partial x_i} \overline{P} + \nu \frac{\partial^2}{\partial x_\alpha \partial x_\alpha} \overline{U}_i, \tag{3a}$$

$$\frac{\partial}{\partial x_\alpha} \overline{U}_\alpha = 0, \tag{3b}$$

$$\partial_t R_{i,j} + R_{\alpha,j} \frac{\partial}{\partial r_\alpha^A} \overline{U}_i(\boldsymbol{r}^A, t) + R_{i,\alpha} \frac{\partial}{\partial r_\alpha^B} \overline{U}_j(\boldsymbol{r}^B, t) + [\overline{U}_\alpha(\boldsymbol{r}^B, t) - \overline{U}_\alpha(\boldsymbol{r}^A, t)]\partial_\alpha R_{i,j}$$

$$= -\partial_\alpha (S_{i,\alpha j} - S_{i\alpha,j}) + \frac{1}{\rho}(\partial_i K_{p,j} - \partial_j K_{i,p}) + 2\nu \partial_\alpha \partial_\alpha R_{i,j} \tag{3c}$$

$$\partial_\alpha R_{\alpha,i} = 0, \quad \partial_\alpha S_{ij,\alpha} = 0, \quad \partial_\alpha K_{p,\alpha} = 0. \tag{3d,e,f}$$

In the above equations $\boldsymbol{r}^A$ and $\boldsymbol{r}^B$ are positions of two arbitrary points A and B within the fluid, whereas $\boldsymbol{r} = \boldsymbol{r}^A - \boldsymbol{r}^B$ and the operator $\partial_i \equiv \partial/\partial r_i$. Furthermore we define the two-point double-velocity, pressure–velocity and triple-velocity correlation functions according to

$$R_{i,j}(\boldsymbol{r}, t) = \overline{u_i^A u_j^B}, \tag{4}$$

$$K_{p,j}(\boldsymbol{r}, t) = \overline{p^A u_j^B}, \tag{5}$$

$$S_{ij,k}(\boldsymbol{r}, t) = \overline{u_i^A u_j^A u_k^B}. \tag{6}$$

Note that the condition of homogeneity imposed on the turbulent field requires that the mean velocity satisfies the relation

$$\overline{U}_i(\boldsymbol{x}) - \overline{U}_i(\boldsymbol{x}^0) = \overline{U}_i(\boldsymbol{x} - \boldsymbol{x}^0), \tag{7}$$

where $\boldsymbol{x}^0$ is an arbitrary fixed point within the fluid and velocity $\overline{U}_i(0) = 0$, which is always attainable by proper Galilean transformation of the velocity field.

The pressure–velocity correlation $K_{p,i}$ may be expressed in terms of the triple-velocity correlation by employing the well-known formula for the pressure field in terms of the velocity field:

$$K_{p,i}(\boldsymbol{r}, t) = \frac{\rho}{4\pi} \int \frac{\mathrm{d}^3 x}{|\boldsymbol{x} - \boldsymbol{r}|} \frac{\partial^2}{\partial x_\alpha \partial x_\beta} S_{\alpha\beta,i}(\boldsymbol{x}, t). \tag{8}$$

Equations (3*a–f*) and (8) contain more quantities than the number of equations, and hence are not closed. We now seek closure for (3*c*), which requires a relation for $S_{ij,k}$ in terms of $R_{i,j}$.

If the tensor $S_{ij,k}$ is to obey condition (3*e*) it has to be in the form of the curl of another tensor:

$$S_{ij,k} = \epsilon_{klm} \partial_l A_{mij}. \tag{9}$$

Since the tensor ϵ_{klm} is not invariant under reflections, the tensor A_{mij} must contain another ϵ_{ijk} to ensure the axisymmetric invariance of $S_{ij,k}$. We may generally write

$$A_{mij} = \epsilon_{mis} B_{sj} + \epsilon_{mjs} B_{si} + \epsilon_{mrs} C_{rsij} + \epsilon_{irs} C'_{rsmj} + \epsilon_{jrs} C'_{rsmi} + \epsilon_{prs} D_{prsmij}, \tag{10}$$

where B, C, D and C' are, as yet, unknown axisymmetrically invariant tensors. Note that the form (10) of A assures the evident symmetry

$$S_{ij,k} = S_{ji,k}. \tag{11}$$

Closure of the set of equations (3) requires us to choose a relation between $S_{ij,k}$ and $R_{i,j}$. A first choice is to neglect higher-order terms, so that

$$B_{ij} = -A(r, t) R_{i,j}, \tag{12a}$$

$$C = C' = 0, \tag{12b}$$

$$D = 0, \tag{12c}$$

where $A(r, t)$ is a scalar function and the minus sign is introduced for later convenience. As we shall see, this closure assumption is equivalent to an eddy-viscosity coefficient concept in the two-point turbulence equations. Equations (9), (10) and (12) yield

$$S_{ij,k} = -\delta_{ki} R_{s,j} \partial_s A + \partial_i A R_{k,j} + (i \leftrightarrow j). \tag{13}$$

From this point we impose the restriction of isotropy. For isotropic turbulence triple- and double-correlation tensors are expressible in terms of the scalar functions k and f related to each other by the Kármán–Howarth equation, which may be derived from (3) (Batchelor 1953; Hinze 1959). Thus

$$\partial_t(\overline{u^2} f) = \frac{1}{r^4} \partial_r(r^4 (\overline{u^2})^{\frac{3}{2}} k) + \frac{2\nu}{r^4} \partial_r(r^4 \partial_r \overline{u^2} f), \tag{14}$$

where $r = |\boldsymbol{r}|$ and $\overline{u^2} = \frac{1}{3}\overline{u_i u_i}$. Any element of $S_{ij,k}$ and $R_{i,j}$ may be obtained from k and f; for example $S_{11,1}(r_1, 0, 0) = (\overline{u^2})^{\frac{3}{2}} k(r_1)$ and $R_{1,1}(r_1, 0, 0) = \overline{u^2} f(r_1)$.

The isotropic equivalent of (13) is

$$(\overline{u^2})^{\frac{3}{2}} k = 2A(r,t)\,\partial_r \overline{u^2 f}, \tag{15}$$

which leads to the closed equation for $\overline{u^2 f}$

$$\partial_t(\overline{u^2 f}) = \frac{2}{r^4}\partial_r(\nu_T(r,t)\, r^4\, \partial_r \overline{u^2 f}), \tag{16}$$

where

$$\nu_T(r,t) = \nu + A(r,t), \tag{17}$$

so that we deal with the notion of an eddy-viscosity coefficient for the function $A(r,t)$.

3. Determination of the eddy-viscosity function

For high Reynolds numbers there exists an appreciable inertial subrange of separation distance r, where Kolmogoroff's 1941 similarity theory provides the following explicit expressions for the correlation functions:

$$\overline{u^2 f}(r,t) = \overline{u^2} - 2\alpha\epsilon(t)^{\frac{2}{3}} r^{\frac{2}{3}}, \tag{18}$$

$$(\overline{u^2})^{\frac{3}{2}} k(r,t) = -\tfrac{2}{15}\epsilon(t)\, r, \tag{19}$$

where the energy dissipation rate

$$\epsilon(t) \equiv -\frac{3}{2}\frac{\mathrm{d}\overline{u^2}}{\mathrm{d}t} = 15\,\overline{u^2}(\partial_r^2 f|_{r=0}). \tag{20}$$

The existence of the inertial subrange has been confirmed in numerous experiments and measurements performed in atmospheric and oceanic boundary layers, and includes measurements by Antonia, Satyaprakash & Chambers (1982), Champagne (1978) and Van Atta & Chen (1970). Additional references and a summary of the available experimental data may be found in Yaglom (1981), Dickey & Mellor (1979) and Monin & Yaglom (1975). Equations (15), (18) and (19) immediately yield the eddy-viscosity coefficient in the inertial subrange

$$\nu_T = \nu + \gamma\epsilon^{\frac{1}{3}} r^{\frac{4}{3}}, \tag{21}$$

where

$$\gamma \equiv 0.05/\alpha. \tag{22}$$

Note that the expression (21) is reminiscent of Richardson's law for relative diffusion in a turbulent medium (Lin 1960; Monin & Yaglom 1975; Larcheveque & Lesieur 1981). However, since there does not exist a simple relation between the double-correlation function of the equation (16) and a probability distribution describing the relative diffusion in a turbulent medium, the result (21) must be considered as independent of Richardson's law.

In the case of the high-Reynolds number ($R_\lambda \sim 10^4$) atmospheric-wind correlation-function observations of Van Atta & Chen (1970) and Antonia *et al.* (1982), (18) and (19) fit the data quite well up to the values $r/\eta_K \sim 10^4$, where $\eta_K \equiv (\nu^3/\epsilon)^{\frac{1}{4}}$ is the Kolmogoroff lengthscale. For the Van Atta & Chen experiments $\alpha = 0.73$ (Dickey & Mellor 1979) and for the Antonia *et al.* experiments $\alpha = 0.61$. Therefore for high Reynolds numbers one has $0.068 \lesssim \gamma \lesssim 0.082$.

On the other hand, for the moderate-Reynolds-number ($R_\lambda \sim 10^2$) wind-tunnel data of Stewart & Townsend (1951), an $r^{\frac{2}{3}}$ portion of the correlation functions is virtually non-existent. We have therefore evaluated ν_T directly from their $k(r)$ and

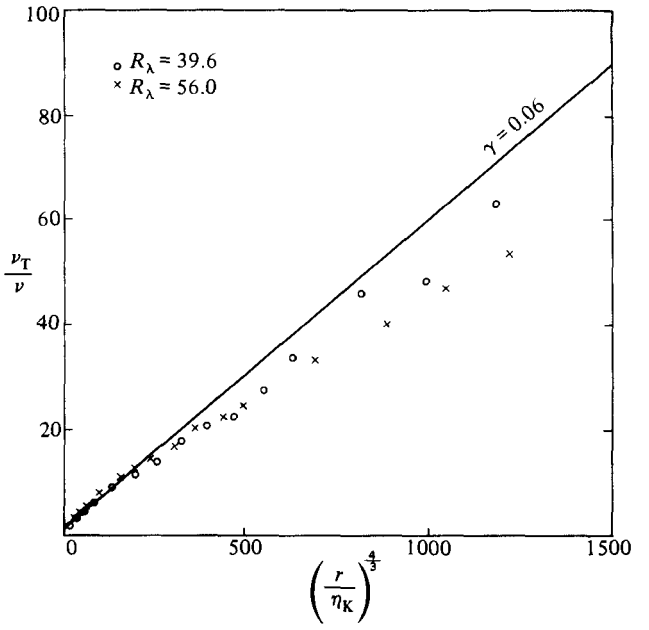

FIGURE 1. Experimental eddy-viscosity coefficient $\nu_T = \nu + \frac{1}{2}(\overline{u^2})^{\frac{1}{2}} k/\partial_r f$ for moderate Reynolds numbers. Data for the double- and triple-correlation functions are from Stewart & Townsend (1951).

$f(r)$ data using (15) and (17). The results are shown in figure 1. Undoubtedly there is error associated with the data and the analysis at large values of r. Nevertheless, the high- and moderate-Reynolds-number results are in fair agreement. Furthermore, the moderate-Reynolds-number data fall roughly on a straight line for large values of r/η_K, where the data have little resemblance to (18) and (19).

We shall see shortly that (21) with $\gamma = 0.06$ is the best choice for moderate-Reynolds-number turbulence (in figure 1, $\gamma = 0.06$ is a compromise value for the range $0 < r/\eta_K < 10^2$). Thus we seemingly obtain a range $0.06 \lesssim \gamma \lesssim 0.08$ for the large-Reynolds-number range $50 \lesssim R_\lambda \lesssim 10^4$.

Formula (21) for the function A does not yield the correct behaviour for the triple-correlation functions for small r. Since $\partial_r f \propto r$ and $A \propto r^{\frac{4}{3}}$ as $r \to 0$, we obtain $k \propto r^{\frac{7}{3}}$ instead of the known behaviour (Hinze 1959) $k \propto r^3$ as $r \to 0$. This feature could be corrected by introducing a more complicated expression for A containing additional disposable constants. However, such corrections should not influence the overall evolution of the turbulence because they are restricted to a negligible region of small r. Therefore, for the present, we adopt the simple form of the eddy-viscosity coefficient given by (21).

The spectral representation of (16) with the eddy-viscosity coefficient (21) is given in Appendix A.

4. Comparison of the theory with experimental results

The range of validity of the hypothesis (21) may be established only by comparison between experimental results and calculations using (21).

Scaling distance, velocity and time by M, ν/M and M^2/ν respectively, where M is any lengthscale encountered in the problem (in laboratory experiments it is usually

the grid mesh size) we obtain the Kármán–Howarth equation in the dimensionless form

$$\partial_t F = \frac{2}{r^4}\partial_r(r^4\partial_r F) + \gamma\left[\frac{15F(0,t)}{[\lambda(t)]^2}\right]^{\frac{1}{3}}\frac{2}{r^4}\partial_r(r^{\frac{16}{3}}\partial_r F). \tag{23}$$

In (23) $F(r,t) = \overline{u^2}f(r,t)$ where $\overline{u^2}$ is non-dimensional, and the non-dimensional Taylor microscale

$$\lambda = -(\partial_r^2 f|_{r=0})^{-\frac{1}{2}}. \tag{24a}$$

Another important parameter is the internal Reynolds number

$$R_\lambda = \lambda(\overline{u^2})^{\frac{1}{2}}. \tag{24b}$$

For the purposes of comparison of the theory with experiments, (23) must be solved numerically. We have used an unconditionally stable implicit central-difference numerical scheme. The boundary conditions imposed on the function $F(r,t)$ are

$$\partial_r F(r,t)|_{r=0} = 0, \tag{25a}$$

$$F(r,t)\to 0 \quad \text{as} \quad r\to\infty. \tag{25b}$$

4.1. *High Reynolds numbers*

By high Reynolds numbers we mean values of the internal Reynolds number R_λ for which there exists an appreciable inertial subrange as given by (18) and (19). According to the experimental data of Antonia *et al.* (1982) and Champagne (1978), we may safely assume that high-Reynolds-number range corresponds to values of R_λ of order 10^3 or greater. Unfortunately, for large Reynolds numbers data on the time evolution of the double-correlation functions have not been reported in the literature. From available experimental data we may only infer that the time evolution of the turbulent field exhibits a Kolmogoroff $r^{\frac{2}{3}}$ law having a range of applicability reduced as the Reynolds number decreases. To see if this behaviour is properly reproduced by (23), it is convenient to look at the time evolution of the normalized dimensionless structure function

$$S(r,t) \equiv \frac{\overline{u^2} - F(r,t)}{(15\overline{u^2}/\lambda^2)^{\frac{1}{2}}} = \frac{R_\lambda}{\sqrt{15}}(1-f(r,t)) \tag{26}$$

containing the inertial $r^{\frac{2}{3}}$ subrange in the initial condition.

The structure function should exhibit the presence of self-preserving inertial subrange at subsequent times, if expressed in terms of r/η_K, where $\eta_K \equiv (15\overline{u^2}/\lambda^2)^{\frac{1}{2}}$ is the Kolmogoroff lengthscale. At the initial instant of time we stipulate $\lambda = 1$ and $R_\lambda = 1.2\times 10^4$ and the simplest $f(r,0)$ containing a $r^{\frac{2}{3}}$ region:

$$f(r,0) = \begin{cases} 1-0.5r^2 & (r \leqslant 0.0756), \\ 1-0.016r^{\frac{2}{3}} & (0.0756 < r \leqslant 494.1), \\ 0 & (494.1 < r) \end{cases} \tag{27}$$

The constants were calculated with $\alpha = 0.61$ given by Antonia *et al.* (1982) for our initial value of R_λ, and the inertial-range curve $r^{\frac{2}{3}}$ is assumed to extend between $r = 0.0756$, where it crosses the parabolic curve valid for small r, and $r = 494.1$, where it is cut off to prevent it from becoming negative.

The results of the time evolution of the initial condition (27) shown in figure 2 properly preserve the inertial $r^{\frac{2}{3}}$ part of the structure functions. The range of applicability of the Kolmogoroff law (18) obtained in the numerical experiment for

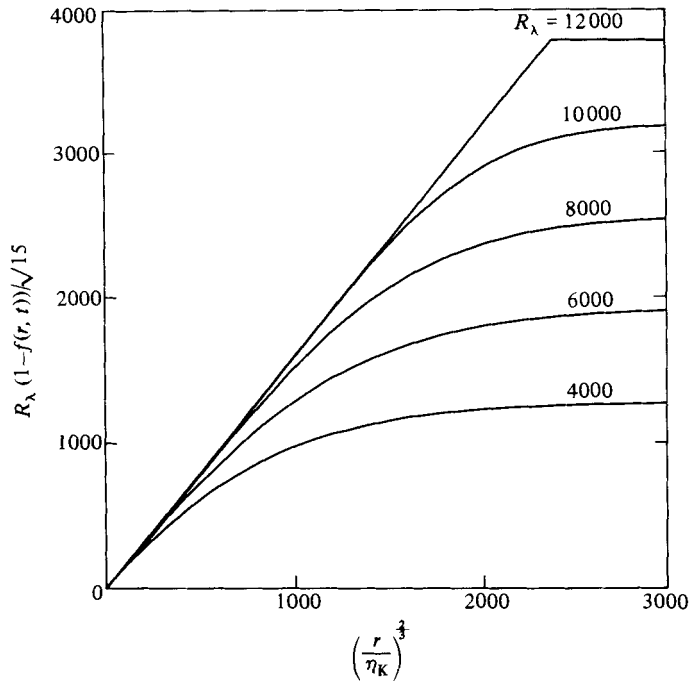

FIGURE 2. Time evolution of the structure function for the initial value of the Reynolds number $R_\lambda = 1.2 \times 10^4$. On the abscissa the variable is $(r/\eta_K)^{\frac{2}{3}}$ where η_K is the Kolmogoroff lengthscale.

$R_\lambda = 8000$ ($(r/\eta_K)^{\frac{2}{3}} \leqslant 10^3$) is in agreement with atmospheric data of Van Atta & Chen (1970) and Antonia *et al.* (1982) for comparable Reynolds numbers.

4.2. *Moderate Reynolds numbers*

For the purpose of comparison of theory and experiments for moderate Reynolds numbers of order 10^2, we chose results of the laboratory experiments performed by Comte-Bellot & Corrsin (1971) and by Dickey & Mellor (1980); the later cover a relatively long decay history.

Comte-Bellot & Corrsin reported results of an experiment performed in a wind tunnel with turbulence generated by a uniform square grid with distance $M = 5.08$ cm between bars. They give values of the decaying double-correlation function at three successive instants of time; some of the properties of the turbulence at these times are summarized in table 1, where all quantities have been transformed to dimensionless form.

The initial condition in the numerical integration of (23) should be the first experimental correlation function, at $t = 1.23 \times 10^{-3}$. However, for the purpose of numerical integration it was necessary to extend the initial values of the correlation function to values of r larger than those where data exist. This turns out to be important in an understanding of the initial period of decay behaviour. Here we describe the mechanics of our procedure, and return to a more extensive discussion in §§5 and 6.

Essentially, the initial profile is the experimental profile, which we extend according to

$$f(r) \propto (r+b)^{-6} \quad (1 \lesssim r \lesssim 20), \tag{28}$$

	$u^2 \times 10^{-3}$		R_λ		λ	
$t \times 10^3$	Observed	Calculated	Observed	Calculated	Observed	Calculated
1.23	570	570	71.6	71.6	0.095	0.095
2.88	190	198	65.3	66.4	0.150	0.159
5.06	93	97	60.7	61.6	0.200	0.207

TABLE 1. Observed and calculated parameters for the experiment of Comte-Bellot & Corrsin (1971); values are non-dimensionalized on M and ν

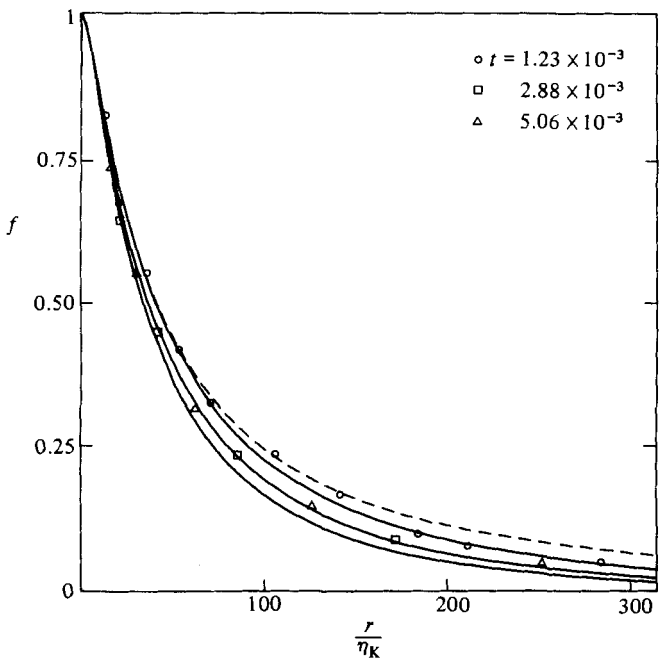

FIGURE 3. Comparison between values of the correlation functions in the Comte-Bellot & Corrsin (1971) experiment and the theoretical predictions. The descending curves are respectively the self-similar solution (dashed line), the experimental initial correlation function at $t = 1.235 \times 10^{-3}$, and the correlation functions at $t = 2.882 \times 10^{-3}$ and $t = 5.058 \times 10^{-3}$ calculated from (23).

where $b = 4.3$ is a matching constant. Equation (28) is in accordance with the finding of Batchelor & Proudman (1956) concerning large-r behaviour of correlation functions in isotropic turbulence. For $r > 20$ the correlation function was set to zero. Equation (23) was then integrated for $\Delta t = 0.001$ to remove the kink at the matching junction; the integral was then reinitiated with the initial $\overline{u^2}$ and λ at $t = 1.23 \times 10^{-3}$. Equation (23) was again numerically integrated with this initial condition using the value $\gamma = 0.06$ inferred from the experiment of Stewart & Townsend (1951). The time evolution of the correlation functions, the turbulent energy decay and the time dependence of the internal Reynolds number are shown in figures 3, 4 and 5 respectively (self-similar solutions discussed in §5 are also depicted in these figures). Some of the calculated turbulence parameters are included in table 1.

Dickey & Mellor (1980) reported results of the laboratory experiments on decaying turbulence in neutral and stratified fluids, which extend for times considerably longer

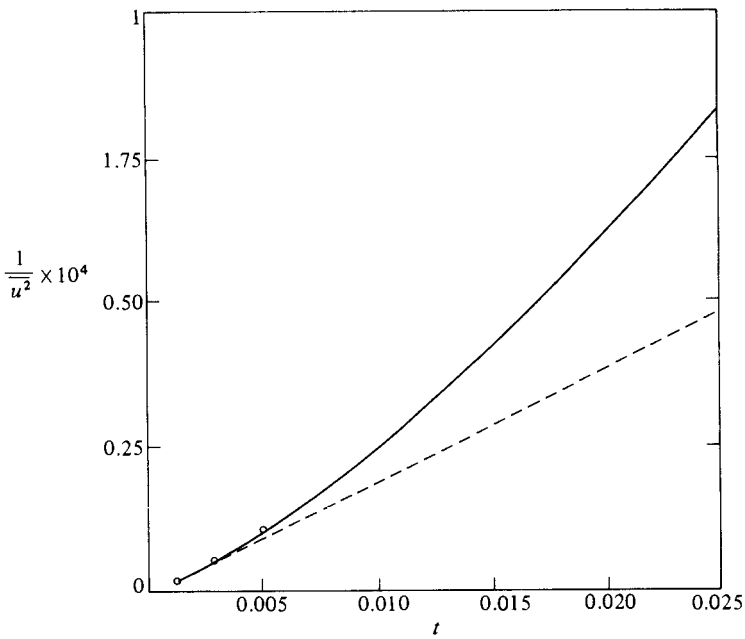

FIGURE 4. Energy decay curves derived from (23) with the experimental (solid line) and self-similar (dashed line) initial conditions. The experimental points are from table 1.

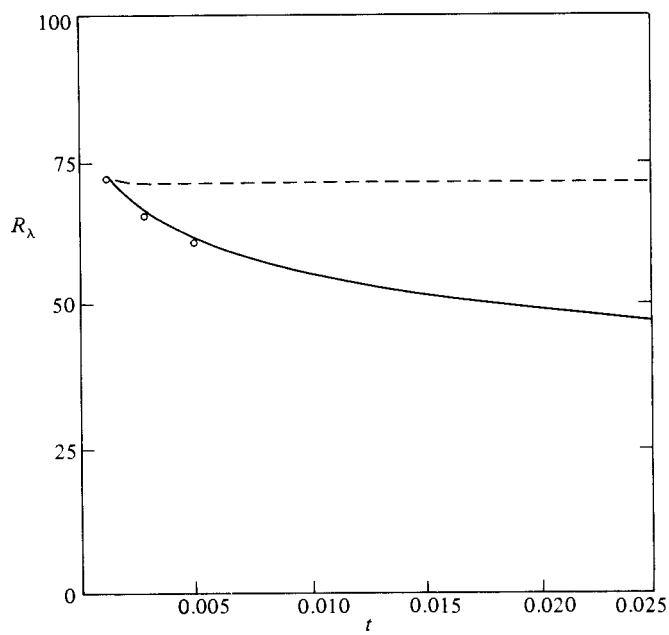

FIGURE 5. Time dependence of the internal Reynolds number for the experimental (solid line) and self-similar (dashed line) initial conditions. The experimental points are from table 1.

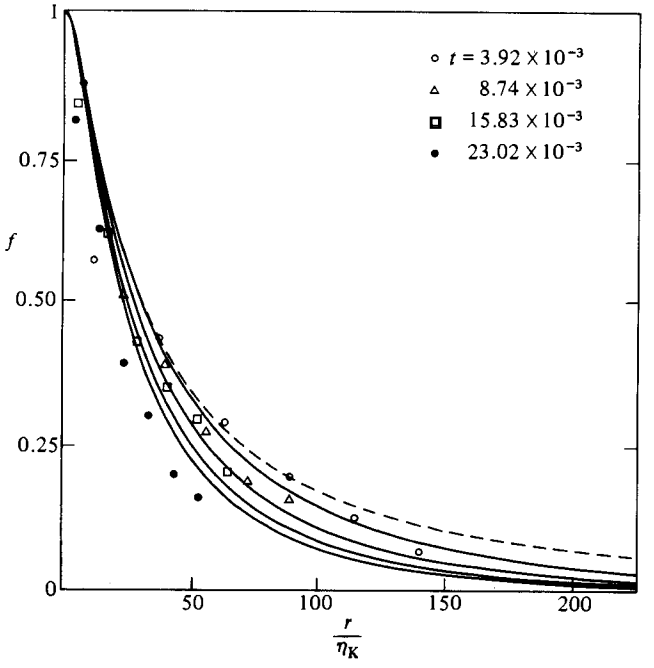

FIGURE 6. Comparison between the correlation functions in the Dickey & Mellor (1980) experiment and the theoretical predictions. The descending curves are respectively the self-similar solution (dashed line), the experimental initial condition at $t = 3.92 \times 10^{-3}$ and the correlation functions at $t = 8.74 \times 10^{-3}$, $t = 15.83 \times 10^{-3}$ and $t = 23.02 \times 10^{-3}$ calculated from (23).

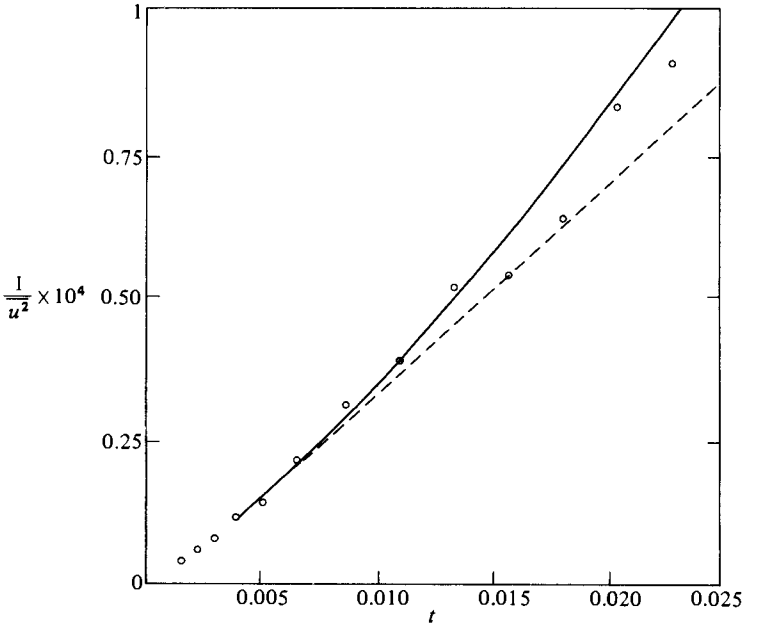

FIGURE 7. Energy-decay curves derived from (23) with the experimental (solid line) and self-similar (dashed line) initial conditions of the Dickey & Mellor (1980) experiment.

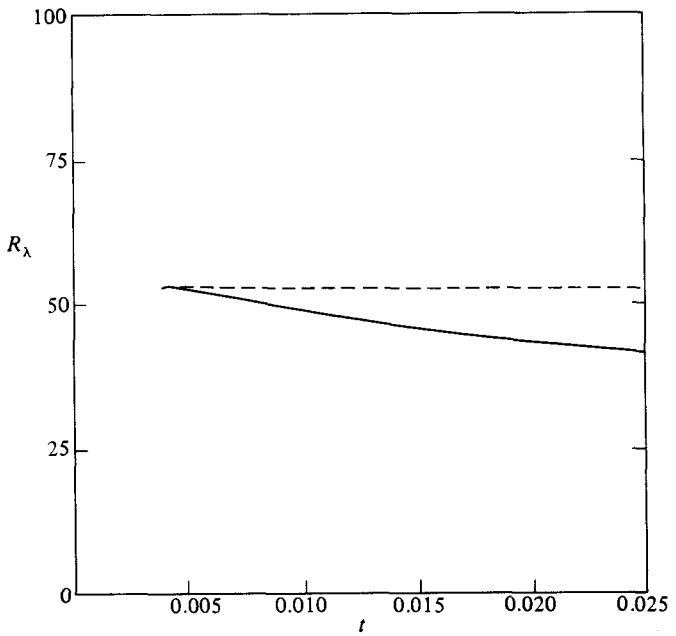

FIGURE 8. Time dependence of the internal Reynolds number for the experimental (solid line) and self-similar (dashed line) initial conditions of the Dickey & Mellor (1980) experiment.

than previous measurements for the same Reynolds numbers (however, the correlation function data were subject to more uncertainty than previous data). They give values of the evolving correlation function at four different instants of time for dimensionless distances $r < 2.5$. As before, the correlation function, fitted to the experimental data at time $t = 3.92 \times 10^{-3}$, was taken as an initial condition and was extended beyond the experimental range with the aid of (28), where $b = 3.4$. The initial Taylor microscale $\lambda = 0.1796$ and the initial internal Reynolds number $R_\lambda = 53$.

The results of the numerical integration of (25) with $\gamma = 0.06$ yield correlation functions, energy decay and the Reynolds number as a function of time shown in figures 6, 7 and 8, respectively.

Note that the correlation-function data in the Dickey & Mellor experiment cover the relatively long time interval $\Delta t = 0.0193$, whereas in the Comte-Bellot & Corrsin experiment (1971) $\Delta t = 0.0038$.

The comparison of calculated values and experimental data is quite favourable.

5. Self-similar solutions

The experimental results on the decay of the turbulent energy for moderate Reynolds numbers are usually represented by a power law (Hinze 1959; Monin & Yaglom 1975)

$$\overline{u^2} \propto t^{-a}, \tag{29}$$

with the exponent somewhat greater or equal to unity. For example, exponents for solid curves in figures 6 and 7 are 1.28 and 1.22 respectively. The values of the exponent a and the constants of proportionality for different experiments may be found in Dickey & Mellor (1980). The decay law with an exponent close to unity persists only for the limited initial interval of time, with the a eventually approaching

the value 2.5 according to Batchelor & Townsend (1948), when the inertial effects become negligible. The decay laws with $a = \frac{10}{7}$ and $\frac{6}{5}$ were derived by Kolmogoroff (1941) and Saffman (1967) respectively. They assumed self-preservation of the correlation functions outside the viscous range; Kolmogoroff also assumed that the Loitsyanskii integral is finite and invariant, implying $f(r,t) = o(r^{-5})$ as $r \to \infty$, whereas Saffman assumed that $f(r,t) = O(r^{-3})$ as $r \to \infty$. Lesieur & Schertzer (1978) investigated the problem of decaying turbulence in the framework of the eddy-damped quasinormal approximation. In the limit of vanishing viscosity they obtained the general result that for the energy spectrum $E(k) \propto k^s$ as $k \to 0$ and $s < 4$ the exponent $a = 2(s+1)/(s+3)$ (for $s = 1$ the assumption of zero viscosity may be discarded). Since there is a one-to-one correspondence between the series expansion of $E(k,t)$ around $k = 0$ and the asymptotic expansion of $f(r,t)$ as $r \to \infty$ (Lighthill 1958), these results show that the energy decay rate is closely related to the large-r behaviour of the correlation functions. It is also well known that the initial period of decay with $a = 1$ may be deduced directly from the Kármán–Howarth equation by assuming self-preservation in time of the double- and triple-correlation functions for all r. It seems interesting to investigate properties of such self-similar correlation functions and their relation to correlation functions found in laboratory experiments.

To establish properties of self-similar solutions to the Kármán–Howarth equation in Kolmogoroff-lengthscale units, we let

$$F(r,t) = \epsilon^{\frac{1}{2}} \Phi(\eta, t), \tag{30}$$

where $\eta \equiv r/\eta_{\mathrm{K}}$, and in the dimensionless units used

$$\eta_{\mathrm{K}} \equiv \epsilon^{-\frac{1}{4}} = \left(\frac{15\overline{u^2}}{\lambda^2}\right)^{-\frac{1}{4}}. \tag{31}$$

If we insert (30) into (23) we obtain

$$\frac{1}{2\epsilon^{\frac{1}{2}}} \partial_t \Phi = \frac{1}{\eta^4}[\eta^4(1+\gamma\eta^{\frac{4}{3}})\partial_\eta \Phi] + E\left(\frac{\eta}{2}\partial_\eta \Phi + \Phi\right), \tag{32}$$

where $E = -\frac{1}{4}\dot{\epsilon}/\epsilon^{\frac{3}{2}}$. Thus far, (32) is simply another form of (23).

The condition of self-similarity, $\Phi = \Phi(\eta)$, requires that $\partial_t \Phi = 0$ and $E = \text{const}$. The latter fact yields $\epsilon \propto t^{-2}$ and $\overline{u^2} \propto t^{-1}$, the so-called initial period of decay law. Specifically, it may be shown that $E = \frac{1}{3}\Phi(0)^{-1} = \frac{1}{3}\sqrt{15}\, R_\lambda^{-1}$.

Equation (32) in this case suggests that $\Phi \propto \eta^{-2}$ for $\eta \to \infty$. The exact solutions of (32) with $\partial_t \Phi = 0$ for two limiting cases $\gamma = 0$ and $\gamma\eta^{\frac{4}{3}} \gg 1$ are given in Appendix B and confirm this suggestion. We may note here that this result is independent of the exact form of the eddy-viscosity function ν_{T} as long as it grows slower than r^2 for large r, and the function Φ is assumed to behave according to the power law r^{-b} at infinity. The asymptotic behaviour of $\Phi \propto r^{-2}$ as $r \to \infty$ is consistent with the behaviour of the energy spectrum $E(k) \propto k$ as $k \to 0$. This may be shown using expression (A 6) of Appendix A with the partition of the domain of integration over k into two subintervals $0 \leqslant k \leqslant k_0$ and $k_0 < k \leqslant \infty$, with k_0 close to $k = 0$.

Using (32) (with $\partial_t \Phi = 0$), self-similar solutions normalized by $\Phi(0) = 1$ for a range of R_λ were numerically generated by means of the Runge–Kutta fourth-order scheme, and are plotted in the form of structure functions in figure 9. The tendency of the structure functions towards Kolmogoroff's curve for large R_λ is explained in Appendix C, where we show that in the limit $R_\lambda \to \infty$ (32) predicts $r^{\frac{2}{3}}$ behaviour of the structure functions outside the viscous range. Other solutions corresponding to the appropriate Reynolds numbers have already been included in figures 3 and 6, and

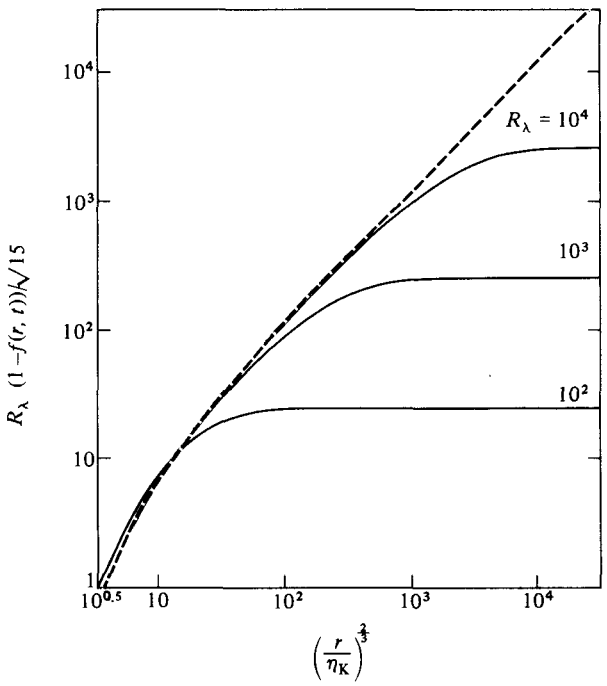

FIGURE 9. Structure function $S = \sqrt{\frac{1}{15}}\, R_\lambda(1-f(r,t))$ for self-similar solutions for different values of R_λ. For moderate Reynolds number $R_\lambda = 10^2$ the value $\gamma = 0.06$, whereas for $R_\lambda = 10^3$ and 10^4 $\gamma = 0.08$. The dashed curve represents (C 6).

their time evolution is depicted in figures 3–8 for comparison with evolving non-self-similar solutions.

Despite fairly good agreement between initial values of the self-similar correlation functions and experimental points, the time evolution is not predicted well. The divergence between time evolution of the self-similar solutions and the experimental results is due to the large-r, r^{-2} behaviour of the former. For real isotropic turbulence, at least

$$f(r,t) = O(r^{-4}) \quad \text{as} \quad r \to \infty \tag{33}$$

(Hinze 1959), and, according to Batchelor & Proudman (1956), correlation functions approach zero even faster.

6. Discussion

We have constructed a two-point turbulence model based on a simple eddy-viscosity closure of the Kármán–Howarth equation in real space coordinates. The closure assumption is a result of the empirical observation that the relation (15) between double- and triple-correlation functions is the same as between correlation functions in the inertial subrange of the Kolmogoroff 1941 theory, even if the Reynolds numbers are too low for the Kolmogoroff theory itself to hold. This observation yields the expression (21) for an eddy-viscosity function applicable for both high and moderate Reynolds numbers. It should be stressed here that the expression (21) for the eddy viscosity is basically empirical and it remains to determine a class of physical processes which are accounted for by this closure. It would also be interesting to investigate a possibility of deriving (23) from the more elaborate spectral closures.

The closed Kármán–Howarth equation (23) forms a simple numerical problem, requiring modest computational time. Results of the numerical calculations compare favourably with experiments.

In the framework of the theory the self-similar solutions of (23) have been investigated. The condition of self-similarity yields the initial-period decay law and the r^{-2} behaviour of the correlation functions for large r. These results are in agreement with previously published results concerning the properties of the energy spectrum which is initially linear in wavenumber k for small k. The self-similar solutions approximate properly the experimental correlation functions through an extensive part of the experimental range for moderate Reynolds numbers, and yield Kolmogoroff's law for large Reynolds numbers. However, they represent poorly the decay of real turbulence because of inadequate modelling of large scales of turbulence.

We are grateful to one of the referees for critical comments which helped us to improve §5. Our thanks go also to Mrs Johann Callan for typing and to Mr William Ellis, Mr Philip Tunison and Mr Michael Zadworney for drawing the figures. The work of J.A.D. was supported by the Geophysical Fluid Dynamics Program, NOAA/ Princeton University Grant 04-7-022-44017.

Appendix A

Most of the existing closure schemes for isotropic turbulence are expressed in terms of spectral quantities (see Rose & Sulem 1971). For that reason it seems worth while to give the spectral counterpart of (16). The spectral equation corresponding to (30) for isotropic turbulence reads

$$\partial_t E(k,t) = F(k,t) - 2\nu k^2 E(k,t), \tag{A 1}$$

where

$$E(k,t) = \frac{1}{\pi}\int_0^\infty \mathrm{d}r\, kr \sin kr R_{\alpha,\alpha}(r,t), \tag{A 2}$$

$$F(k,t) = \frac{2}{\pi}\int_0^\infty \mathrm{d}r\, kr \sin kr\, \partial_\alpha S_{\alpha\beta,\beta}. \tag{A 3}$$

For isotropic turbulence we show easily that

$$\partial_\alpha S_{\alpha\beta,\beta} = \overline{u^2}\frac{1}{r^4}\partial_r(r^4 A\, \partial_r f). \tag{A 4}$$

Inserting the above expression into (A 3) and assuming that the double-correlation function f goes to zero sufficiently quickly with increasing r, we integrate twice by parts, arriving at the relation

$$\begin{aligned} F(k,t) = -\gamma\Big[\int_0^\infty \mathrm{d}k' 2\nu k'^2 E(k',t)\Big]^{\frac{1}{3}} \\ \times\frac{4}{\pi}\int_0^\infty \mathrm{d}r \int_0^\infty \mathrm{d}k' kr^{\frac{4}{3}}\Big(\frac{4\sin kr}{r} + k^2 r\sin kr + \tfrac{2}{3}k\cos kr\Big) \\ \times\Big(\frac{\cos k'r}{k'^2 r^2} - \frac{\sin k'r}{k'^3 r^3}\Big)E(k',t). \end{aligned} \tag{A 5}$$

In deriving (A 5), the spectral representation of f,

$$\overline{u^2}f = 2\int_0^\infty \mathrm{d}k' \left(\frac{\sin k'r}{k'^3r^3} - \frac{\cos k'r}{k'^2r^2}\right) E(k',t), \tag{A 6}$$

was used. Note that in (A 5) integrals over the variables r and k are not interchangeable.

Appendix B

Equation (32) with $\partial_t \Phi$ and γ set to zero was solved by the Frobenius (power-series) method, providing the solution

$$\Phi(\eta) = \frac{6\Phi(0)}{E}\left[\frac{1}{\eta^2} - \left(\frac{4}{E}\right)^{\frac{1}{2}}\frac{1}{\eta^3}\exp\left(-\frac{E\eta^2}{4}\right)\mathrm{erfi}\left(\left(\frac{E}{4}\right)^{\frac{1}{2}}\eta\right)\right], \tag{B 1}$$

where

$$\mathrm{erfi}\,(x) \equiv \int_0^x \mathrm{e}^{t^2}\,\mathrm{d}t. \tag{B 2}$$

We show easily that

$$\Phi(\eta) \to \mathrm{const} \equiv \Phi(0) \quad \text{as} \quad \eta \to 0, \tag{B 3}$$

$$\Phi'(0) = 0, \tag{B 4}$$

$$\Phi''(0) = \frac{-\Phi(0)}{\sqrt{15}\,R_\lambda}. \tag{B 5}$$

The asymptotic expansion of the function erfi gives behaviour of $\Phi(\eta)$ for large values of the variable η:

$$\Phi(\eta) \underset{\eta\to\infty}{\approx} \frac{6\Phi(0)}{E}\left(\frac{1}{\eta^2} - \frac{2}{E}\frac{1}{\eta^4} - \frac{4}{E^2}\frac{1}{\eta^6} + \ldots\right). \tag{B 6}$$

The leading term in (B 6) is $1/\eta^2$. To obtain solution of (32) for large η and $\gamma \neq 0$, we transform the variables in (32)

$$\eta = x^{\frac{3}{2}}, \tag{B 7}$$

arriving at

$$4(x+\gamma x^3)\,\Phi''(x) + (22 + 30\gamma x^2 + 3Ex^3)\,\Phi'(x) + 9Ex^2\Phi(x) = 0. \tag{B 8}$$

Neglecting the viscous terms in (B 8), we obtain the familiar confluent hypergeometric equation

$$z\Phi''(z) + (c-z)\,\Phi'(z) - a\Phi(z) = 0, \tag{B 9}$$

where

$$z = -\frac{0.75E}{\gamma}x, \quad c = 7.5, \quad a = 3.$$

The solution of (B 9) that is regular at $z = 0$ approximates the solution of the full equation (B 8) for large values of the variable x. The asymptotic expansion of the confluent hypergeometric function for large negative z is

$$\Phi(a,c;z) = \frac{\Gamma(c)}{\Gamma(c-a)}(-z)^{-a}\left(1 + O\left(\frac{1}{z}\right)\right) \tag{B 10}$$

(Dingle 1973), giving again the behaviour of the correlation function inversely proportional to η^2 for large η.

Appendix C

A case of theoretical interest is the limit $R_\lambda \to \infty$, where we expect Kolmogoroff's law (18) to be valid for an extensive range of r. In this limit, (32), with $\partial_t \Phi = 0$ and ϕ normalized by $\phi(0) = 1$, yields as the only physically acceptable solution

$$\Phi(\eta) = 1, \tag{C 1}$$

which is not of great interest.

For large values of R_λ it is more convenient to consider the equation for the self-similar structure function $S(\eta; R_\lambda) \equiv R_\lambda(1-\Phi(\eta; R_\lambda))/\sqrt{15} \equiv R_\lambda \psi(\eta; R_\lambda)/\sqrt{15}$, where $0 \leqslant \psi \leqslant 1$. The equation for ψ is a simple consequence of (32):

$$\frac{R_\lambda}{\sqrt{15}} \frac{1}{\eta^4} \frac{\mathrm{d}}{\mathrm{d}\eta}\left[\eta^4(1+\gamma\eta^{\frac{4}{3}}) \frac{\mathrm{d}\psi}{\mathrm{d}\eta}\right] + \frac{1}{3}\left[\frac{\eta}{2}\frac{\mathrm{d}\psi}{\mathrm{d}\eta} + \psi - 1\right] = 0. \tag{C 2}$$

In the limit $R_\lambda \to \infty$ the second term in (C 2) is bounded and non-zero (it could be zero for $\psi = A\eta^{-2}+1$, which is infinite for $\eta = 0$), and to satisfy (C 2) we must have

$$\psi(\eta; R_\lambda) = O\left(\frac{1}{R_\lambda}\right) \quad \text{as} \quad R_\lambda \to \infty. \tag{C 3}$$

Therefore for large R_λ we may write

$$\psi(\eta; R_\lambda) = \frac{1}{R_\lambda} \psi_1(\eta; R_\lambda), \tag{C 4}$$

where ψ_1 has the finite non-zero limit $\overline{\psi}_1(\eta) = \sqrt{15}\, S(\eta; \infty)$ for each $\eta \neq 0$ if $R_\lambda \to \infty$. This conclusion may be easily checked on a specific example of the exact solution to (C 2) given in Appendix B. From (C 2) and (C 4) the equation for $S(\eta; \infty)$ is

$$\frac{\mathrm{d}}{\mathrm{d}\eta}\left[\eta^4(1+\gamma\eta^{\frac{4}{3}}) \frac{\mathrm{d}S}{\mathrm{d}\eta}\right] = \tfrac{1}{3}\eta^4. \tag{C 5}$$

Equation (C 5) has the solution

$$S = \frac{1}{10\gamma}\left(\eta^{\frac{2}{3}} - \frac{1}{\gamma^{\frac{1}{2}}} \arctan\left(\gamma^{\frac{1}{2}}\eta^{\frac{2}{3}}\right)\right). \tag{C 6}$$

For small r we obtain

$$S = \tfrac{1}{30}\eta^2, \tag{C 7}$$

whereas for large r

$$S = 2\alpha\eta^{\frac{2}{3}} - \tfrac{1}{20}\pi\gamma^{-\frac{3}{2}}, \tag{C 8}$$

which is precisely the Kolmogoroff law with the additive constant. A tendency towards establishing the relation (C 8) for structure functions for $R_\lambda \to \infty$ is seen in figure 9, where the dashed line represents expression (C 6) with $\alpha = 0.61$. This value of α was used to generate structure functions of figure 9 numerically for $R_\lambda = 10^3$ and 10^4.

REFERENCES

Antonia, R. A., Satyaprakash, B. R. & Chambers, A. J. 1982 *Phys. Fluids* **25**, 1.

Batchelor, G. K. 1953 *The Theory of Homogeneous Turbulence*. Cambridge University Press.

Batchelor, G. K. & Proudman, I. 1956 *Phil. Trans. R. Soc. Lond.* A **248**, 369.

Batchelor G. K. & Townsend, A. A. 1948 *Proc. R. Soc. Lond* A **199**, 527.

CHAMPAGNE, F. H. 1978 *J. Fluid Mech.* **86**, 67.

COMTE-BELLOT, G. & CORRSIN, S. 1971 *J. Fluid Mech.* **48**, 273.

DICKEY, T. D. & MELLOR, G. L. 1979 *Phys. Fluids* **22**, 1029.

DICKEY, T. D. & MELLOR, G. L. 1980 *J. Fluid Mech.* **99**, 13.

DINGLE, R. B. 1973 *Asymptotic Expansions.* Academic.

HASSELMANN, K. 1958 *Deutsche hydrogr. Z.* **11**, 207.

HINZE, J. O. 1959 *Turbulence.* McGraw-Hill.

KOLMOGOROFF, A. N. 1941 *C.R. Acad. Sci. USSR* **30**, 301.

LARCHEVEQUE, M. & LESIEUR, M. 1981 *J. Méc.* **20**, 113.

LESIEUR, M. & SCHERTZER, D. 1978 *J. Méc.* **17**, 609.

LIGHTHILL, M. J. 1958 *Introduction to Fourier Analysis and Generalized Functions.* Cambridge University Press.

LIN, C. C. 1960 *Proc. NAS* **46**, 566.

MONIN, A. S. & YAGLOM, A. M. 1971 *Statistical Fluid Mechanics: Mechanics of Turbulence*, vol. I. MIT Press.

MONIN, A. S. & YAGLOM, A. M. 1975 *Statistical Fluid Mechanics: Mechanics of Turbulence*, vol. II. MIT Press.

ORSZAG, S. A. 1977 Statistical theory of turbulence. In *Fluid Dynamics: Les Houches 1973* (ed. R. Balian & J.-L. Peube). Gordon & Breach.

ROSE, H. A. & SULEM, P. L. 1978 *J. Phys. (Paris)* **39**, 441.

SAFFMAN, P. G. 1967 *Phys. Fluids* **10**, 1349.

STEWART, R. W. & TOWNSEND, A. A. 1951 *Phil. Trans. R. Soc. Lond.* A **243,** 359.

VAN ATTA, C. W. & CHEN, W. Y. 1970 *J. Fluid Mech.* **44**, 145.

YAGLOM, A. M. 1981 *Izv. Acad. Sci. USSR, Phys. Atmos. Ocean* **17**, 1235 (in Russian).